

An Approach to Robust Synchronization of Electric Power Generators

Olaoluwapo Ajala

Alejandro D. Domínguez-García

Daniel Liberzon

Abstract—We consider the problem of synchronizing two electric power generators, one of which (the leader) is serving a time-varying load, so that they can ultimately be connected to form a single power system. Both generators are described by second-order reduced state-space models, and we assume that the generator not serving any load initially (the follower) has access to measurements of the leader generator phase angle corrupted by some additive disturbances. By using these measurements, and leveraging results on reduced-order observers with ISS-type robustness, we propose a procedure that drives (i) the angular velocity of the follower close enough to that of the leader, and (ii) the phase angle of the follower close enough to that of the point at which both systems will be electrically connected. An explicit bound on the synchronization error in terms of the measurement disturbance and the variations in the electrical load served by the leader is computed. We illustrate the procedure via numerical simulations.

I. INTRODUCTION

Research into synchronization of dynamical systems originates in the 17th century study of pendulum clocks by Huygens and continues vigorously to this day, driven by theoretical interest and applications in mechanical and electrical systems, multi-agent coordination, teleoperation, haptics, and other fields. In the physics literature, the famous Pecora-Carroll synchronization scheme from [1] has generated a lot of activity, some of which was recently surveyed in [2]. In modern control-theoretic literature, tools that have been prominent in addressing synchronization problems are dissipativity theory [3]–[5] and observer design [6]–[8]. In the context of electric power systems, Kuramoto-type models of coupled phase oscillators, which have been utilized in numerous areas since first proposed in [9], are also starting to be adopted to describe the behavior of inertia-less microgrids (see, e.g., [10]–[13] and the references therein).

In this paper, we consider two power systems that are not electrically connected, with the ultimate goal of interconnecting them to form a single system with all its generators being synchronized, i.e., rotating at the same angular velocity. Here, we focus on the case when the first system, referred to as the leader, is comprised of one generator and one load, both of which are connected to a bus with voltage support; and the second system, referred to as the follower system,

Olaoluwapo Ajala and Alejandro D. Domínguez-García are with the Department of Electrical and Computer Engineering, University of Illinois at Urbana-Champaign, Urbana, IL 61801, U.S.A. Their work was supported by the Advanced Research Projects Agency-Energy (ARPA-E), U.S. Department of Energy, within the NODES program, under Award DE-AR0000695. E-mail: {ooajala2,aledan@ILLINOIS.EDU.

Daniel Liberzon is with the Coordinated Science Laboratory, University of Illinois at Urbana-Champaign, Urbana, IL 61801, U.S.A. His work was supported by the NSF grant CMMI-1662708 and the AFOSR grant FA9550-17-1-0236. E-mail: liberzon@ILLINOIS.EDU.

is comprised of a single generator. The objective then is to synchronize both systems, i.e., make the generators rotate at the same angular velocity, and make the phase angle of the point at which they will be interconnected match. Once these two objectives are achieved, it is possible to electrically connect the follower system to the leader system without causing large currents to flow across both systems, or causing mechanical components to break (see, e.g., [14]).

By assuming the load in the leader system is not varying too rapidly, we first show that a standard integral control stabilizes the angular velocity of the generator in the leader system. Then, by assuming the follower system has access to measurements of the phase of the generator in the leader system, we can show that even if these measurements are corrupted, due to, e.g., noise or a malicious cyber attack, the generator in the follower system will be able to bring its angular velocity close enough to the angular velocity of the generator in the leader system. As for phase synchronization, our procedure cannot guarantee that the phase difference will converge to within some small value around zero; in fact, the opposite is generally true—the phase difference will grow unbounded over time. It turns out, however, that this is not a problem in practice, since one just needs to wait until the phase difference is a multiple of 2π to physically interconnect both systems.

While the setting considered here might seem at first too simplistic, we believe it is of interest in some emerging applications, namely microgrids. In such applications, one can think of the generator in the leader system model considered in this paper as an aggregate model describing, e.g., the average dynamics of a collection of generators in the microgrid that are already synchronized and serving a collection of loads (one can think of the sum of these loads as the load in the leader system). In this setting, the problem is to synchronize one additional generator (the follower system in the context of this work) to those in the microgrid that are already synchronized.

II. SYSTEM DESCRIPTION

We focus on the task of synchronizing two generators, with the first one serving a load via a node referred to as the “bus,” as depicted in Fig. 1, and the second one trying to connect to the bus.

Let ω_1 denote the angular speed of the first generator (in electrical radians per second), let θ_1 denote the absolute phase angle of generator 1, and let δ_1 denote its relative phase angle, both in radians. This means that

$$\delta_1 := \theta_1 - \omega_0 t, \quad (1)$$

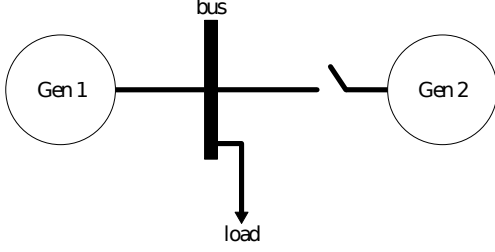


Fig. 1. Synchronization of two generators: a leader and a follower.

where ω_0 denotes some nominal frequency; thus, we have $\dot{\theta}_1 = \omega_1$, so that

$$\dot{\delta}_1 = \omega_1 - \omega_0. \quad (2)$$

The corresponding variables $\omega_2, \theta_2, \delta_2$ for the second generator are defined in the same way. The bus state variables are the voltage magnitude and the voltage angle for the bus. We denote by θ_3 the absolute phase angle of the bus voltage. We also define the relative phase angle of the bus voltage as

$$\delta_3 := \theta_3 - \omega_0 t, \quad (3)$$

and we have $\dot{\theta}_3 = \omega_3$, so that $\dot{\delta}_3 = \omega_3 - \omega_0$, where ω_3 is the frequency of the bus (in electrical radians per second).

We consider the following second-order reduced model for the first generator (see [15] for the details of its derivation):

$$\dot{\theta}_1 = \omega_1, \quad (4)$$

$$\dot{\omega}_1 = u_1 - \ell(t) - D_1^{(0)} \omega_1, \quad (5)$$

where u_1 is the control input (which corresponds to the mechanical power applied to the generator shaft);

$$\ell(t) = B_1(\theta_{13}(t)) + D_1(\theta_{13}(t)) \cdot \dot{\theta}_{13}(t) \quad (6)$$

is the power consumed by the electrical load connected to the bus,

$$\theta_{13}(t) := \theta_1(t) - \theta_3(t) \quad (7)$$

is the difference between the absolute phase angles of the first generator and the bus; B_1 is a globally bounded and globally Lipschitz function taking values

$$B_1(s) := K_1 \sin(s) + X_1 \sin(2s), \quad (8)$$

where K_1 is a positive constant, and X_1 is a nonnegative constant [15]; the damping function D_1 is a globally bounded and globally Lipschitz function taking values

$$D_1(s) = C_1 \cos^2(s) + C_2 \sin^2(s) \quad (9)$$

where C_1 and C_2 are nonnegative constants [15]; and $D_1^{(0)}$ is a positive constant.

From the generator dynamic model in (4), (5), and the definition (7) and the resulting relation

$$\begin{aligned} \dot{\theta}_{13}(t) &:= \dot{\theta}_1(t) - \dot{\theta}_3(t) \\ &= \omega_1 - \omega_3, \end{aligned} \quad (10)$$

it is easy to see that the dynamical model for the bus takes the form

$$\dot{\theta}_3 = \omega_3, \quad (11)$$

$$\dot{\omega}_3 = u_1 - \ell(t) - D_1^{(0)} \omega_1 - \ddot{\theta}_{13}(t). \quad (12)$$

The second-order reduced model for the second generator (before it is connected) is analogous to (4), (5) but with no electrical load term, i.e.,

$$\dot{\theta}_2 = \omega_2, \quad (13)$$

$$\dot{\omega}_2 = u_2 - D_2^{(0)} \omega_2, \quad (14)$$

where u_2 is the control input and $D_2^{(0)}$ is a positive constant.

The synchronization task consists in ensuring that the phase and angular speed of the second generator match those of the bus. Accordingly, from now on we refer to the bus modeled by (11), (12) as the *leader*, and the second generator modeled by (13), (14) as the *follower*.

We assume that at the initial time t_0 (the time when our control strategy will be initialized), the first generator operates in steady state corresponding to some constant load $\bar{\ell}$. In view of the power balance equation (6), this means that $\theta_{13}(t_0)$ equals the solution $\bar{\theta}_{13}$ of the equation $\bar{\ell} = B_1(\bar{\theta}_{13})$, and that $\dot{\theta}_{13}(t_0) = \omega_1(t_0) - \omega_3(t_0) = 0$. [Indeed, $\theta_{13}(t) \equiv \bar{\theta}_{13}$ is the unique solution of the ODE $\dot{\bar{\ell}} = B_1(\theta_{13}(t)) + D_1(\theta_{13}(t)) \cdot \dot{\theta}_{13}(t)$ starting at $\bar{\theta}_{13}$.]

For $t \geq t_0$, we allow the load $\ell(t)$ to change, but assume that this change is constrained both in size and in speed, i.e., we assume that for some positive constants Δ_ℓ and $\Delta_{\dot{\ell}}$ we have

$$|\ell(t) - \bar{\ell}| \leq \Delta_\ell, \quad |\dot{\ell}(t)| \leq \Delta_{\dot{\ell}}. \quad (15)$$

By small-signal analysis, one can show that if Δ_ℓ and $\Delta_{\dot{\ell}}$ are sufficiently small then, at least on some finite time horizon, there exist positive constants Δ_θ and $\Delta_{\dot{\theta}}$ such that

$$|\theta_{13}(t) - \bar{\theta}_{13}| \leq \Delta_\theta, \quad |\dot{\theta}_{13}(t)| = |\omega_1(t) - \omega_3(t)| \leq \Delta_{\dot{\theta}}. \quad (16)$$

We henceforth assume the existence of such constants Δ_θ and $\Delta_{\dot{\theta}}$.

Signal measurements: We assume that a phasor-measurement unit (PMU) is used to measure the absolute angle $\theta_3(t)$ of the “bus” node, but that these measurements are corrupted by a measurement disturbance, $d(t)$. One major potential source of such a disturbance is *spoofing* [16], but it can also be due to a combination of several sources. Thus, phase measurements available to the follower take the form

$$\theta_3(t) + d(t), \quad (17)$$

where $d(t)$ is an unknown disturbance, with $\theta_3(t) + d(t) \in [0, 2\pi)$.¹ We also assume that the steady-state value $\bar{\theta}_{13}$ is

¹Note that if the unknown disturbance is caused by a spoofing attack on the GPS receiving of the PMU, it might be possible to refine the upper bound on $d(t)$. For example, in [16], it was shown that a spoofing attack can be engineered so as to perturb the phase measurement provided by the PMU by as much as 0.25π rad without being detected; thus, in such a case, one could assume $d(t) \in (-0.25\pi, 0.25\pi)$.

known to the follower (through the knowledge of $\bar{\ell}$.) On the other hand, angular speed measurements are not available to the follower.

Our goal is to achieve robust synchronization in the face of the unknown disturbance d , and to quantitatively characterize how the synchronization error is affected by the size of this disturbance.

III. CONTROLLED SYNCHRONIZATION

In this section, a feedback control law is designed for the leader and a synchronization method is developed for the follower system.

A. Control design and analysis

First generator and bus (leader): Note that the first generator and the bus share the same control input. The purpose of this control is to drive the bus frequency $\omega_3(t)$ to the nominal frequency value ω_0 . In view of the second bound in (16), if $\Delta_{\dot{\theta}}$ is small then this goal can also be approximately achieved by driving the angular speed $\omega_1(t)$ of the first generator to ω_0 . This suggests the following control input:

$$u_1(t) = -k\delta_1(t) = -k(\theta_1(t) - \omega_0 t), \quad k > 0. \quad (18)$$

Since the dynamics of $\delta_1(t)$ are given by (2), it is easy to recognize in (18) a standard integral control law for making $\omega_1(t)$ asymptotically track the constant reference ω_0 . Under the action of this control, the first generator reduced-order model (4), (5) becomes:

$$\dot{\theta}_1 = \omega_1, \quad (19)$$

$$\dot{\omega}_1 = -k\theta_1 + k\omega_0 t - \ell(t) - D_1^{(0)}\omega_1. \quad (20)$$

To validate the control law (18), we want to show that the solutions of the closed-loop system given by (2), (19) and (20) are bounded and that $\omega_1(t)$ is regulated to ω_0 in an appropriate sense. To this end, it is convenient to rewrite the (ω_1, δ_1) -dynamics as follows:

$$\begin{pmatrix} \dot{\omega}_1 \\ \dot{\delta}_1 \end{pmatrix} = \begin{pmatrix} -D_1^{(0)} & -k \\ 1 & 0 \end{pmatrix} \begin{pmatrix} \omega_1 \\ \delta_1 \end{pmatrix} - \begin{pmatrix} \ell(t) \\ \omega_0 \end{pmatrix},$$

which we can view as a linear time-invariant system driven by a time-varying perturbation that creates a time-varying equilibrium at

$$\omega_1 = \omega_0, \quad \delta_1 = -\frac{\ell(t) + D_1^{(0)}\omega_0}{k} =: \delta_0(t) \quad (21)$$

(meaning that for each frozen time t , this is the equilibrium of the corresponding fixed affine system). Let us shift the center of coordinates to this time-varying equilibrium by defining

$$\bar{\omega}_1(t) := \omega_1(t) - \omega_0, \quad \bar{\delta}_1(t) := \delta_1(t) - \delta_0(t).$$

In these new coordinates, the closed-loop dynamics becomes:

$$\begin{pmatrix} \dot{\bar{\omega}}_1 \\ \dot{\bar{\delta}}_1 \end{pmatrix} = \begin{pmatrix} \dot{\omega}_1 \\ \dot{\delta}_1 \end{pmatrix} - \begin{pmatrix} 0 \\ \dot{\delta}_0(t) \end{pmatrix}$$

$$= \begin{pmatrix} -D_1^{(0)} & -k \\ 1 & 0 \end{pmatrix} \begin{pmatrix} \bar{\omega}_1 \\ \bar{\delta}_1 \end{pmatrix} + \begin{pmatrix} 0 \\ \nu(t) \end{pmatrix}, \quad (22)$$

where

$$\nu(t) := \frac{\dot{\ell}(t)}{k}. \quad (23)$$

Since the matrix

$$A := \begin{pmatrix} -D_1^{(0)} & -k \\ 1 & 0 \end{pmatrix} \quad (24)$$

is Hurwitz for every $k > 0$, it is clear that closed-loop solutions are bounded and converge to a neighborhood of the time-varying equilibrium (21); the size of this neighborhood is determined by the size of the perturbation $\nu(t)$. To make this more precise, note that since A is Hurwitz, there exist constants $c, \lambda > 0$ such that for all t we have²

$$\|e^{At}\| \leq ce^{-\lambda t}. \quad (25)$$

Our system (22) is the LTI system $\dot{x} = Ax$ driven by the perturbation (23) which, in view of the second bound in (15), satisfies

$$|\nu(t)| \leq \frac{\Delta_{\dot{\ell}}}{k} \quad \forall t \geq 0.$$

It is well known and straightforward to derive that c/λ is the system's \mathcal{L}_∞ -induced gain, and that the following bound holds for all solutions:

$$\left| \begin{pmatrix} \bar{\omega}_1(t) \\ \bar{\delta}_1(t) \end{pmatrix} \right| \leq ce^{-\lambda t} \left| \begin{pmatrix} \bar{\omega}_1(0) \\ \bar{\delta}_1(0) \end{pmatrix} \right| + \frac{c}{\lambda} \frac{\Delta_{\dot{\ell}}}{k} \quad \forall t \geq 0.$$

In particular, $c\Delta_{\dot{\ell}}/(\lambda k)$ is the ultimate bound on the norm of the solution in steady state:

$$\limsup_{t \rightarrow \infty} \left| \begin{pmatrix} \bar{\omega}_1(t) \\ \bar{\delta}_1(t) \end{pmatrix} \right| \leq \frac{c\Delta_{\dot{\ell}}}{\lambda k}. \quad (26)$$

Note that small values of $\bar{\omega}_1(t)$ correspond to $\omega_1(t)$ being regulated close to the nominal frequency ω_0 .

Second generator (follower): For the follower (second generator) described by (13), (14), we would like to define the control input $u_2(t)$ so as to make the angular speed $\omega_2(t)$ synchronize with the bus frequency $\omega_3(t)$. Since in view of the second bound in (16) the frequencies $\omega_3(t)$ and $\omega_1(t)$ are close to each other, it is reasonable to base the design of u_2 on the (somewhat simpler) dynamics of the first generator instead of those of the bus. Let us use (6) to rewrite the equation (20) as

$$\dot{\omega}_1 = -k\theta_1 + k\omega_0 t - B_1(\theta_{13}(t)) - D_1(\theta_{13}(t)) \cdot \dot{\theta}_{13} - D_1^{(0)}\omega_1. \quad (27)$$

We can make the dynamics (14) of ω_2 approximately match these dynamics of ω_1 by doing the following: (i) approximating $\theta_1(t)$, which is not available to the follower, by $\theta_3(t) + d(t) + \bar{\theta}_{13}$. This is reasonable since $\theta_3(t) + d(t)$ is the approximate measurement of $\theta_3(t)$, available to the follower,

²Here $\|\cdot\|$ stands for the induced matrix norm corresponding to the Euclidean norm.

and $\bar{\theta}_{13}$ approximates the difference $\theta_{13}(t) = \theta_1(t) - \theta_3(t)$ in the sense of the first bound in (16), and is also available to the follower; (ii) approximating $B_1(\theta_{13}(t))$ by $B_1(\bar{\theta}_{13})$; (iii) correcting the difference between the damping constants $D_1^{(0)}$ and $D_2^{(0)}$; and (iv) ignoring the term $D_1(\theta_{13}(t)) \cdot \dot{\theta}_{13}$ which is bounded by virtue of (9) and (16). This suggests the following control input:

$$u_2(t) = -k(\theta_3(t) + d(t) + \bar{\theta}_{13}) + k\omega_0 t - B_1(\bar{\theta}_{13}) + (D_2^{(0)} - D_1^{(0)})\omega_2(t).$$

We can then write the closed-loop dynamics of the follower as

$$\dot{\theta}_2 = \omega_2, \quad (28)$$

$$\begin{aligned} \dot{\omega}_2 = & -k(\theta_3(t) + d(t) + \bar{\theta}_{13}) + k\omega_0 t - B_1(\bar{\theta}_{13}) \\ & - D_1^{(0)}\omega_2. \end{aligned} \quad (29)$$

This choice of control for the follower will be validated by the synchronization analysis given next.

Remark 1 The above control design for the follower is not dependent on the particular form of the control u_1 for the leader, but only on the fact that this control depends just on the angle θ_1 and not on the angular velocity ω_1 . We also see that the exact nature of the damping term in the follower model is not important because it is canceled by control.

B. Synchronization analysis

Since we are interested in synchronizing the angular velocity ω_2 of the follower to the frequency ω_3 of the leader, we consider the synchronization error

$$e(t) := \omega_2(t) - \omega_3(t). \quad (30)$$

We find it convenient to split it as

$$e = (\omega_2 - \omega_1) + (\omega_1 - \omega_3) =: e_{21} + e_{13} \quad (31)$$

and analyze the two components separately. For e_{13} , we already have the second bound from (16) which says that

$$|e_{13}(t)| \leq \Delta_{\dot{\theta}}. \quad (32)$$

For e_{21} , using (29), (27), and (7) we have (suppressing all time arguments for simplicity)

$$\begin{aligned} \dot{e}_{21} = \dot{\omega}_2 - \dot{\omega}_1 = & B_1(\theta_{13}) - B_1(\bar{\theta}_{13}) + D_1(\theta_{13}) \cdot \dot{\theta}_{13} \\ & - D_1^{(0)}e_{21} + k(\theta_{13} - \bar{\theta}_{13}) - kd. \end{aligned} \quad (33)$$

Let us define the candidate Lyapunov function

$$V(e_{21}) := \frac{1}{2}e_{21}^2.$$

Its derivative along solutions of (33) satisfies the inequality

$$\begin{aligned} \dot{V} \leq & -D_1^{(0)}e_{21}^2 + \left(k|\theta_{13} - \bar{\theta}_{13}| + k|d| + |B_1(\theta_{13}) \right. \\ & \left. - B_1(\bar{\theta}_{13})| + |D_1(\theta_{13}) \cdot \dot{\theta}_{13}| \right) |e_{21}|. \end{aligned} \quad (34)$$

Recall that $D_1^{(0)} > 0$, and by the first bound in (16) we have $|\theta_{13} - \bar{\theta}_{13}| \leq \Delta_{\theta}$. Furthermore, since B_1 defined in (8)

is globally Lipschitz with Lipschitz constant $K_1 + 2X_1$, we also have $|B_1(\theta_{13}) - B_1(\bar{\theta}_{13})| \leq (K_1 + 2X_1)\Delta_{\theta}$. Finally, D_1 defined in (9) is globally bounded by $C_1 + C_2$ which, combined with the second bound in (16), gives $|D_1(\theta_{13}) \cdot \dot{\theta}_{13}| \leq (C_1 + C_2)\Delta_{\dot{\theta}}$. Plugging all these bounds into (34), we obtain

$$\begin{aligned} \dot{V} \leq & -D_1^{(0)}e_{21}^2 + \left(k|d| + (k + K_1 + 2X_1)\Delta_{\theta} \right. \\ & \left. + (C_1 + C_2)\Delta_{\dot{\theta}} \right) |e_{21}| \\ = & -D_1^{(0)}|e_{21}| \left(|e_{21}| \right. \\ & \left. - \frac{k|d| + (k + K_1 + 2X_1)\Delta_{\theta} + (C_1 + C_2)\Delta_{\dot{\theta}}}{D_1^{(0)}} \right), \end{aligned}$$

which yields

$$\begin{aligned} |e_{21}| & > \frac{k|d| + (k + K_1 + 2X_1)\Delta_{\theta} + (C_1 + C_2)\Delta_{\dot{\theta}}}{D_1^{(0)}} \\ \Rightarrow \dot{V} & < 0. \end{aligned}$$

The standard ISS analysis (see, e.g., [17]) now implies that $e_{21}(t)$ stays bounded and satisfies the ultimate bound

$$\begin{aligned} \limsup_{t \rightarrow \infty} |e_{21}(t)| \leq & \frac{1}{D_1^{(0)}} \left(k \limsup_{t \rightarrow \infty} |d(t)| + (C_1 + C_2)\Delta_{\dot{\theta}} \right. \\ & \left. + (k + K_1 + 2X_1)\Delta_{\theta} \right). \end{aligned}$$

Combining this with (31) and (32), we conclude that

$$\begin{aligned} \limsup_{t \rightarrow \infty} |e(t)| \leq & \frac{1}{D_1^{(0)}} \left(k \limsup_{t \rightarrow \infty} |d(t)| + (C_1 + C_2 \right. \\ & \left. + D_1^{(0)})\Delta_{\dot{\theta}} + (k + K_1 + 2X_1)\Delta_{\theta} \right). \end{aligned} \quad (35)$$

This characterizes the quality of synchronization in terms of the size of the disturbance $d(t)$, the control gain k , and the various constants appearing on the right-hand side of (35). The above reasoning and conclusion can be viewed as a special case of the results in [18] on reduced-order observers with ISS-type robustness.

We see, in particular, that the gain from the measurement disturbance d to the synchronization error e is proportional to the control gain k , thus decreasing k reduces the effect of this disturbance on synchronization. On the other hand, decreasing k has a negative effect on closed-loop stability of the first generator, as can be seen from the eigenvalues of the matrix A defined in (24) and from the bound (26). This suggests that, to mitigate the effect of this disturbance, we may want to (temporarily) reduce the control gain k during the synchronization stage.

Synchronization procedure: In addition to angular velocity synchronization, phase synchronization is also important. The phase θ_2 will evolve according to (28), which comes from the physics of the system but was not explicitly taken into account in the above procedure. Due to the ‘‘drift’’ in the frequency caused by the disturbances, there will be a time when θ_2 will become close to θ_3 . The idea is that we will detect when this happens by looking at the measurements

$\theta_3 + d$, and at that moment, we will connect the second generator.

It is important to note that for $|d| > 0.055\pi$, the phase synchronization error will exceed standard error bounds listed in [14], and given that $d(t) \in (-0.25\pi, 0.25\pi)$, it is clear that disturbances could lead to poor synchronization. Although we are aware of this issue, it is beyond the scope of this paper but will be addressed in a future work.

IV. NUMERICAL RESULTS

In this section, parameters for the proposed control law and synchronization method are evaluated, and numerical validations of both techniques are presented. The numerical results are developed as follows: with initial conditions of the leader system set to an equilibrium state and that of the follower system set to zero, the simulations starts at time $t = 0$ s with the electrical load $\ell(t)$ at a nominal value of 0.5 pu, where ‘‘pu’’ denotes per-unit.³ At time $t = 5$ s, the load is perturbed about the nominal value, with the change in size and speed constrained to $|\ell(t) - 0.5| \leq \Delta_\ell$ and $|\dot{\ell}(t)| = \Delta_{\dot{\ell}}$, respectively, where Δ_ℓ and $\Delta_{\dot{\ell}}$ are positive constants. Using a base power of 835 MW for the system, a base voltage amplitude of 26 kV for the generators, and a base voltage amplitude of 230 kV for the bus, the parameter values used are: $k = 0.0008$, $\omega_0 = 120\pi$ rad/s, $D_1^{(0)} = D_2^{(0)} = 0.0265$ s/rad, $\bar{\ell} = 0.5$ pu, $K_1 = 0.7475$ pu, $X_1 = 0$ pu, $C_1 = 1.4643$ pu, and $C_2 = 0.0738$ pu.

A. Parameter evaluation

The values of λ and c in (25) can be easily estimated as follows. The eigenvalues of A are

$$\lambda_{1,2}(A) = \frac{-D_1^{(0)} \pm \sqrt{(D_1^{(0)})^2 - 4k}}{2}.$$

To simplify calculations, let us assume that the control gain is chosen to satisfy $k \geq (D_1^{(0)})^2/4$ so that the eigenvalues of A are complex with real parts $-\frac{1}{2}D_1^{(0)}$. Then, we can take the stability margin (i.e., exponential decay rate) λ appearing in (25) to be

$$\lambda := \frac{1}{2}D_1^{(0)}.$$

(Note that for values of k closer to 0 the stability margin would decrease.) To calculate the overshoot constant c in (25), we can look for a matrix $P = P^T > 0$ which satisfies the Lyapunov inequality

$$PA + A^T P \leq -2\lambda P. \quad (36)$$

Then, A has its overshoot constant c upper-bounded by $\sqrt{\lambda_{\max}(P)/\lambda_{\min}(P)}$. It can be verified that one choice of P satisfying (36) is

$$P = \begin{pmatrix} 1 & \frac{1}{2}D_1^{(0)} \\ \frac{1}{2}D_1^{(0)} & k \end{pmatrix}$$

³System quantities expressed in per-unit have been normalized as fractions of a defined base quantity, and the system rated value is usually chosen as the base quantity. In other words, for a system whose rated power capacity is 10 W, a power measurement of 0.5 pu is equivalent to 5 W [19].

(this actually gives $PA + A^T P = -D_1^{(0)}P$). Its eigenvalues are

$$\lambda_{1,2}(P) = \frac{k + 1 \pm \sqrt{(k-1)^2 + (D_1^{(0)})^2}}{2}.$$

If we fix some value of control gain $k > (D_1^{(0)})^2/4$ (strict inequality is needed to have $P > 0$), we obtain the following estimate for c :

$$c = \sqrt{\frac{k + 1 + \sqrt{(k-1)^2 + (D_1^{(0)})^2}}{k + 1 - \sqrt{(k-1)^2 + (D_1^{(0)})^2}}}.$$

(To refine this result, one could search for a matrix P that gives the smallest value of c .) In the results presented, $c = 40.0361$ and $\lambda = 0.0133$ is used.

B. Control performance analysis

For the leader to be in compliance with the IEEE 1547 standard [20], we must have that $|\omega_3(t) - \omega_0| \leq \pi$ rad/s enforced throughout system operation. Accordingly, effects of various model parameters on control performance were analyzed numerically.

As depicted in Fig. 2, the system frequency deviation from nominal value is investigated and compared to the bound $|\omega_3(t) - \omega_0| \leq \pi$ rad/s required by the IEEE 1547 standard. The control performance results show that increasing values of Δ_ℓ negatively impact the control performance under the integral control. Also, numerical results are presented, in Figs. 3 and 4, to validate the analytical result in (26). For all values of k and $\Delta_{\dot{\ell}}$ considered, it follows that $\left| \begin{matrix} \bar{\omega}_1(t) \\ \bar{\delta}_1(t) \end{matrix} \right| < \frac{c\Delta_{\dot{\ell}}}{\lambda k}$. Although this theoretical bound appears to be very conservative, the norm of the states is observed to be within these bounds, as expected.

C. Synchronization performance analysis

Due to the ISS properties established above, the frequencies ω_3 and ω_2 will synchronize up to an error, as shown in (35). In line with IEEE standards listed in [14], the largest admissible synchronization error, i.e. $e(t) = |\omega_2 - \omega_3|$, is 0.134π rad/s, and this must be enforced before the leader and follower can be interconnected. Accordingly, the effects of disturbance $d(t)$ and control gain k on the synchronization error are investigated via numerical simulations. By utilizing results in [16] for the maximum phase angle error resulting from spoofing attacks, i.e. $d(t) \in (-0.25\pi, 0.25\pi)$ rad, and simulating the effects of increasing k on the synchronization error, we were able to observe and estimate upper bounds for k below which $e(t) \leq 0.134\pi$ rad/s, and acceptable synchronization is achieved.

The numerical results depicted in Fig. 5 show that the proposed synchronization method is robust to large disturbances in phase measurements, even if the disturbance is twice as large as the maximum resulting from spoofing attacks, as reported in [16]. Also, increasing the control gain k improves controller performance (see Fig. 3), but at the cost of reducing robustness of the synchronization method (see Fig. 6).

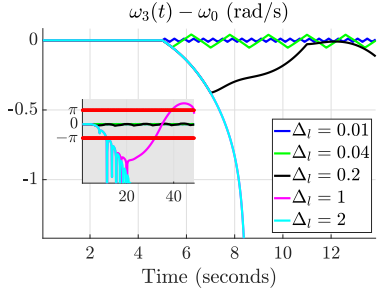


Fig. 2. Frequency deviation ($\Delta_\ell = 0.1$).

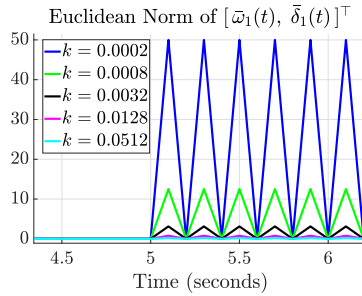


Fig. 3. Norm of states ($\Delta_\ell = 0.01, \Delta_j = 0.1$).

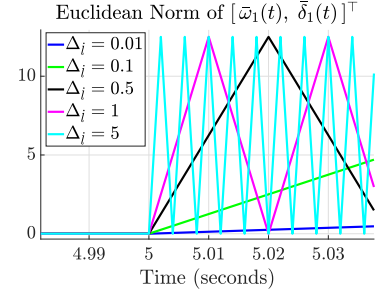


Fig. 4. Norm of states ($k = 8e^{-4}, \Delta_\ell = 0.01$).

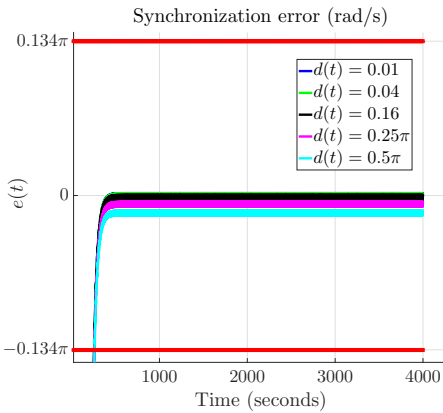


Fig. 5. Synchronization error $e(t)$, for $k = 0.0008, 0.01 \leq d(t) \leq 0.5\pi$.

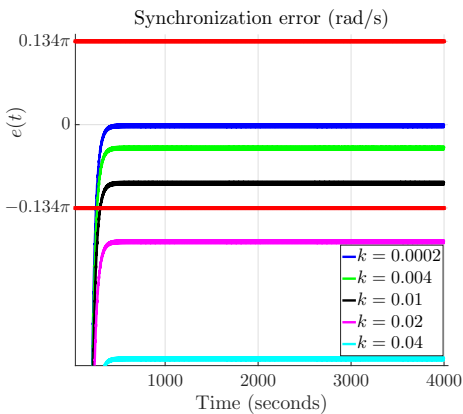


Fig. 6. Synchronization error $e(t)$, for $d(t) = 0.25\pi, 0.0002 \leq k \leq 0.04\pi$.

V. CONCLUDING REMARKS

In this paper, we proposed a method for synchronizing two electric power generators, which is robust against disturbances in the measurements on which the method relies. Analytical and numerical results were used to validate the proposed robust synchronization method.

REFERENCES

[1] L. M. Pecora and T. L. Carroll, "Synchronization in chaotic systems," *Phys. Rev. Lett.*, vol. 64, pp. 821–823, 1990.

[2] L. M. Pecora and T. L. Carroll, "Synchronization of chaotic systems," *Chaos: An Interdisciplinary Journal of Nonlinear Science*, vol. 25, no. 9, p. 097611, 2015.

[3] M. Arcak, "Passivity as a design tool for group coordination," *IEEE Transactions on Automatic Control*, vol. 52, pp. 1380–1390, 2007.

[4] B. Andrievskii and A. L. Fradkov, "Method of passification in adaptive control, estimation, and synchronization," *Autom. Remote Control*, vol. 67, pp. 1699–1731, 2006.

[5] N. Chopra, M. W. Spong, and R. Lozano, "Synchronization of bilateral teleoperators with time delay," *Automatica*, vol. 44, pp. 2142–2148, 2008.

[6] H. Nijmeijer and I. Mareels, "An observer looks at synchronization," vol. 44, pp. 882–890, 1997.

[7] A. Pogromsky and H. Nijmeijer, "Observer-based robust synchronization of dynamical systems," *Int. J. Bifurcation and Chaos in Applied Sciences and Engineering*, vol. 8, pp. 2243–2254, 1998.

[8] B. Andrievsky, A. L. Fradkov, and D. Liberzon, "Robustness of Pecora-Carroll synchronization under communication constraints," *Systems Control Lett.*, vol. 111, pp. 27–33, 2017.

[9] Y. Kuramoto, "Self-entrainment of a population of coupled non-linear oscillators," in *International Symposium on Mathematical Problems in Theoretical Physics*, H. Araki, Ed. Berlin, Heidelberg: Springer Berlin Heidelberg, 1975, pp. 420–422.

[10] F. Dörfler and F. Bullo, "Synchronization in complex networks of phase oscillators: a survey," *Automatica*, vol. 50, pp. 1539–1564, 2014.

[11] F. Dörfler, J. W. Simpson-Porco, and F. Bullo, "Breaking the hierarchy: Distributed control and economic optimality in microgrids," *IEEE Transactions on Control of Network Systems*, vol. 3, no. 3, pp. 241–253, Sept 2016.

[12] J. W. Simpson-Porco, F. Dörfler, and F. Bullo, "Synchronization and power sharing for droop-controlled inverters in islanded microgrids," *Automatica*, vol. 49, no. 9, pp. 2603 – 2611, 2013.

[13] M. Zholbaryssov and A. D. Domínguez-García, "Exploiting phase cohesiveness for frequency control of islanded inverter-based microgrids," in *Proc. IEEE Conference on Decision and Control*, Dec 2016, pp. 4214–4219.

[14] M. J. Thompson, "Fundamentals and advancements in generator synchronizing systems," in *Proc. Annual Conference for Protective Relay Engineers*, Apr. 2012, pp. 203–214.

[15] O. Ajala, A. Domínguez-García, P. Sauer, and D. Liberzon. (2018) A library of second-order models for synchronous machines. [Online]. Available: <https://arxiv.org/abs/1803.09707>

[16] X. Jiang, J. Zhang, B. J. Harding, J. J. Makela, and A. D. Domínguez-García, "Spoofing GPS receiver clock offset of phasor measurement units," *IEEE Transactions on Power Systems*, vol. 28, no. 3, pp. 3253–3262, Aug 2013.

[17] E. D. Sontag, "Smooth stabilization implies coprime factorization," *IEEE Transactions on Automatic Control*, vol. 34, pp. 435–443, 1989.

[18] H. Shim and D. Liberzon, "Nonlinear observers robust to measurement disturbances in an ISS sense," vol. 61, pp. 48–61, 2016.

[19] P. Kundur, N. J. Balu, and M. G. Lauby, *Power System Stability and Control*. McGraw-Hill, 1994.

[20] "IEEE Application Guide for IEEE Std 1547(TM), IEEE Standard for Interconnecting Distributed Resources with Electric Power Systems," *IEEE Std 1547.2-2008*, pp. 1–217, April 2009.